ISSN 1070-3284, Russian Journal of Coordination Chemistry, 2023, Vol. 49, No. 10, pp. 660–671. © Pleiades Publishing, Ltd., 2023.
Russian Text © The Author(s), 2023, published in Koordinatsionnaya Khimiya, 2023, Vol. 49, No. 10, pp. 632–643.

Copper(II) Furancarboxylate Complexes with 5-Nitro-1,10-Phenanthroline as Promising Biological Agents

K. A. Koshenskova[a], D. E. Baravikov[a, b], Yu. V. Nelyubina[c], P. V. Primakov[c], V. O. Shender[d], I. K. Maljants[d], O. B. Bekker[e], T. M. Aliev[c], E. A. Borodin[f], D. D. Kotel'nikov[f], N. Yu. Leusova[g], S. N. Mantrov[b], M. A. Kiskin[a], I. L. Eremenko[a, c], and I. A. Lutsenko[a, *]

[a] *Kurnakov Institute of General and Inorganic Chemistry, Russian Academy of Sciences, Moscow, Russia*
[b] *Mendeleev University of Chemical Technology of Russia, Moscow, Russia*
[c] *Nesmeyanov Institute of Organoelement Compounds, Russian Academy of Sciences, Moscow, Russia*
[d] *Lopukhin Federal Research and Clinical Center of Physical Chemical Medicine, Federal Medical Biological Agency, Moscow, Russia*
[e] *Vavilov Institute of General Genetics, Russian Academy of Sciences, Moscow, Russia*
[f] *Amur State Medical Academy, Blagoveshchensk, Russia*
[g] *Institute of Geology and Nature Management, Far East Branch, Russian Academy of Sciences, Blagoveshchensk, Russia*
**e-mail: irinalu05@rambler.ru*

Received March 1, 2023; revised April 18, 2023; accepted May 3, 2023

Abstract—The reaction of copper(II) acetate with 2-furancarboxylic (HFur)/5-nitro-2-furancarboxylic (HNfur) acids and 5-nitro-1,10-phenanthroline (Nphen) in methanol resulted in the formation of the binuclear coordination compounds $[Cu_2(L)_4(Nphen)_2]\cdot X$ (L = Fur (**I**), Nfur (**II**); X = H_2O (**I**)), which were structurally studied by direct X-ray diffraction (CCDC no. 2244205 (**I**) and 2244206 (**II**)). According to X-ray diffraction data, the coordination environment of the central metal ion in **I** and **II** is composed of two nitrogen atoms of Nphen and three oxygen atoms of the acid anions, which thus form the $\{CuN_2O_3\}$ tetragonal pyramid in which the copper coordination number is five. Intermolecular hydrogen bonds and stacking interactions between the Nphen aromatic rings provide supramolecular stabilization of **I** and **II**. A characteristic feature of supramolecular organization of **II** is the presence of a coordination bond between the Cu^{2+} cation and oxygen of the Nphen NO_2^- group of parallel chains. A biological activity assay for complexes **I** and **II** concerning the cytotoxic properties against a human ovarian adenocarcinoma cell line (*SKOV3*) and the mycobacterial strain *Mycolicibacterium smegmatis* showed an efficient suppression of cell viability. The results of mathematical modeling of the probability of Cu^{2+} binding to amino acid residues of *M. smegmatis* proteins suggested the affinity of the Cu(II) ion to a number of amino acids in polypeptide sites. It was shown that metal ion binding in mycobacterial proteins is more characteristic of histidine- and glutamic acid-containing moieties.

Keywords: copper(II), coordination compounds, furancarboxylates, 5-nitro-1,10-phenanthroline, crystal structure, biological activity, *Mycolicibacterium smegmatis*, *SKOV3*, mathematical modeling

DOI: 10.1134/S1070328423600730

INTRODUCTION

Metal coordination compounds attract the attention of researchers because of their unique ability to form structures of various size and nuclearity, while the possibility of varying the composition by selecting ligands enables the synthesis of compounds with desired properties [1–3]. Metal complexes have a broad range of practical applications: as dyes and pigments, catalysts, molecular magnets, analytical agents, and fungicides [4–7]. Studies of the last decades are concerned with the potential of using metal complexes in medicine: as contrast agents in magnetic resonance imaging (MRI), as radiopharmaceuticals, and for the treatment of anemia, arthritis, ulcers, etc. [8–11]. The discovery of the highly efficient anticancer agent cisplatin (CP) and the subsequent entry of its analogues into the pharmaceutical market stimulated the study of complexes of various metals (not only platinum group metals) for their potential applicability for the treatment of various types of cancer [12–17]. Currently, phenanthroline complexes of essential (vital) metals (Co, Fe, Zn, Mn, Cu, etc.) are actively investigated as promising biological agents, because it has been repeatedly shown that a tandem of 3d metals with phenanthroline possess antibacterial, antitumor, antiparasitic, and other properties, owing to the ability of the ligand to interact

(intercalate) with DNA molecules [18–26]. For example, a known group of anticarcinogenic agents under the trade name Casiopeinas® based on copper(II) and 2,2'-bipyridine and 1,10-phenanthroline derivatives is in the final stages of clinical trials in Mexico [27–29].

In this study, copper was used as the complex-forming ion; copper is an essential element for living organisms playing a number of vital redox functions. (e.g., respiratory chain electron transport, oxidative phosphorylation, removal of superoxide radicals, etc.) [30–33]. Our previous studies [34–41] of the antibacterial and anticancer activities of Fe(III), Co(II), Ni(II), Cu(II), Zn(II), and other metal furoate complexes with N-donor ligands against a non-pathogenic mycobacterial strain *Mycolicibacterium smegmatis* and ovarian adenocarcinoma cell line (*SKOV3*) demonstrated that the highest activity is inherent in Cu(II) and Au(III) compounds containing a phenanthroline moiety (this fact was also reported in [42, 43]). Therefore, in this study, we describe the procedures for the synthesis of copper(II) complexes with 2-furancarboxylic (HFur) or 5-nitro-2-furancarboxylic (HNfur) acid anion and 5-nitro-1,10-phenanthroline (Nphen): $[Cu_2(Fur)_4(Nphen)_2]\cdot H_2O$ (**I**) and $[Cu_2(Nfur)_4(Nphen)_2]$ (**II**). The structures of the complexes were determined by X-ray diffraction; stability of the complexes upon the dissolution in physiological saline was monitored by UV-Vis spectra, and the biological activity in vitro was determined for *SKOV3* cells and the model non-pathogenic *M. smegmatis* strain. For determining the affinity of Cu^{2+} to some *M. smegmatis* proteins, intermolecular docking was carried out with separation of the potential amino acid groups in polypeptide sequences.

EXPERIMENTAL

The complexes were synthesized in air using distilled water and solvents without further purification, namely, methanol (reagent grade, Khimmed) and acetonitrile (reagent grade, Khimmed). Commercially available chemicals were used for the synthesis: copper(II) acetate monohydrate (95%, Acros), 2-furancarboxylic acid (98%, Acros), 5-nitro-2-furancarboxylic acid (99%, Aldrich), and 5-nitro-1,10-phenanthroline (99%, Fluorochem).

Elemental analysis was performed on a Carlo Erba EA 1108 automated C,H,N-analyzer. IR spectra were recorded on a Perkin-Elmer Spectrum 65 Fourier transform IR spectrophotometer in the attenuated total reflectance (ATR) mode in the 400–4000 cm^{-1} frequency range.

UV-Vis spectra were measured on a Shimadzu UV-2600 spectrophotometer in 0.9% solutions of Solo-Pharm NaCl in the 220–400 nm range. The stability of complexes **I** and **II** in solutions was monitored by measuring the spectra of the sample (50 mm) at room temperature every 6 h over periods of 36 and 48 h, respectively.

The biological activity of **I** and **II** was determined in the *M. smegmatis* mc^2 155 test system by the disc diffusion method using paper discs. The growth inhibition zone of the strain seeded in a lawn on agar medium around paper discs containing a test compound in various concentrations was measured. The bacteria that were washed from the Petri dishes with Tryptone soya agar M-290 (Himedia) were cultured overnight in the Lemco-TW liquid medium (Lab Lemco' Powder 5 g L^{-1} (Oxoid); Peptone special, 5 g L^{-1} (Oxoid); NaCl, 5 g L^{-1}; Tween-80) at +37°C up to the mid-logarithmic growth phase at the optical density OD_{600} of 1.5, and mixed with the molten M-290 agar medium in 1 : 9 : 10 ratio (culture : Lemco-TW : M-290). The culture was incubated for 24 h at +37°C. The compound concentration inducing the minimum inhibition zone was taken as the minimum inhibitory concentration (MIC). The test compounds were applied onto discs in different concentrations and the diameter of the culture growth inhibition zone (halo) was measured.

The cytotoxic effect of various concentrations of **I** and **II** against *SKOV3* and the primary human dermal fibroblast (*HDF*) culture was determined using the MTT assay. The method is based on measurement of the activity of a mitochondrial enzyme, succinate dehydrogenase, and is widely used to evaluate the anticancer activity of potential drugs in vitro. From the MTT assay results, half-maximal inhibitory concentration (IC_{50}) was calculated for both compounds. The *SKOV3* cells were received from the ATCC collection; the primary *HDF* culture was received from a healthy donor. The *SKOV3* and *HDF* cells were cultured in the DMEM medium (10% FBS, 2 mM glutamine, 1% gentamycin). The cells were cultured in plastic vials under sterile conditions; the cells were incubated at 37°C in the presence of 5% CO_2. The stock solutions (50 μM) of compounds **I** and **II** were prepared in DMSO. For the addition to cells, they were diluted to desired concentrations in the *SKOV3* and *HDF* culture medium and seeded into 96-well plates in amounts of 4×10^3 and 3.5×10^3 cells per well, respectively. The cells were allowed to attach for at least 14 h, and then various concentrations of the test compounds or DMSO (as the control) were added by the titration method in three repetitions. The final volume of the medium in the wells was 100 μL. Within 48 h after the addition of the agents, the cell viability was measured using the MTT reagent (Sigma). MTT working solution (7 mg/mL, 10 μL per well) were added into the wells containing the cells (in 100 μL of the medium), incubated for 3 h, and the medium was replaced by a DMSO solution. The absorbance of each well was determined at 570 nm using a plate reader (TECAN Infinite M Plex), and the background absorbance was then subtracted. The concentrations that caused 50%

growth inhibition of cell population (IC_{50}) were determined from the dose-dependent curves.

Synthesis of $[Cu_2(Fur)_4(Nphen)_2]\cdot H_2O$ (I). Weighed amounts of $Cu(OAc)_2\cdot H_2O$ (0.200 g, 1 mmol) and HFur (0.224 g, 2 mmol) were dissolved in MeCN (20 mL). Nphen (0.225 g, 1 mmol) dissolved in MeOH (10 mL) was added to the resulting suspension. The reaction mixture was kept at 70°C for 3 h. The blue solution thus formed was filtered and concentrated to 20 mL, and the mother liquor was kept at room temperature. After a few days, blue crystals were formed, they were separated from the mother liquor by decantation, washed with MeCN, and dried in air. The yield of **I** was 0.42 g (81%).

For $C_{44}H_{28}N_6O_{17}Cu_2$ (**I**)

Anal. calcd., %	C, 50.82	H, 2.71	N, 8.08
Found, %	C, 50.84	H, 2.72	N, 8.12

IR (ATR; ν, cm^{-1}): 3096 br.w, 2972 vw, 2293 vw, 2255 w, 1803 vw, 1598 vs, 1554 s, 1515 vs, 1478 vs, 1401 s, 1347 vs, 1220 m, 1186 s, 1142 m, 1075 m, 1009 s, 930 m, 902 m, 880 m, 832 s, 806 vs, 776 vs, 720 s, 654 m, 614 s, 559 m, 516 m, 469 s, 429 m.

Synthesis of $[Cu_2(Nfur)_4(Nphen)_2]$ (II). Weighed amounts of $Cu(OAc)_2\cdot H_2O$ (0.200 g, 1 mmol) and HNfur (0.314 g, 2 mmol) were dissolved in MeCN (20 mL). Nphen (0.225 g, 1 mmol) dissolved in MeOH (10 mL) was added to the resulting suspension. The reaction mixture was kept at 55°C for 3 h. The resulting blue solution was filtered into a Schlenk vessel and concentrated to 20 mL, and the mother liquor was kept at room temperature. After a few days, turquoise-colored crystals were formed; they were separated from the mother liquor by decantation, washed with MeCN, and dried in air. The yield of **II** was 0.48 g (79%).

For $C_{44}H_{22}N_{10}O_{24}Cu_2$ (**II**)

Anal. calcd., %	C, 43.97	H, 1.85	N, 11.66
Found, %	C, 44.01	H, 1.89	N, 11.59

IR (ATR; ν, cm^{-1}): 3664 br.w, 3119 w, 3086 br.w, 2980 br.w, 2903 br.w, 1638 s, 1575 m, 1522 s, 1422 m, 1393 m, 1318 vs, 1239 m, 1152 m, 1118 m, 1064 m, 1013 m, 960 m, 947 m, 905 m, 829 s, 809 s, 782 vs, 723 s, 646 m, 605 m, 546 m, 516 m, 480 m, 429 m.

X-ray diffraction study of complexes **I** and **II** was carried out at 100 K on a Bruker Apex II DUO diffractometer (CCD array detector, MoK_α radiation, λ = 0.71073 Å, graphite monochromator). The structures were solved using the ShelXT software [44] and refined by the full-matrix least-squares method using the Olex2 software [45] in the anisotropic approximation for non-hydrogen atoms. The hydrogen atoms of the water molecule were located from difference Fourier maps, while positions of other hydrogen atoms were calculated geometrically. All of H atoms were refined in the isotropic approximation using the riding model. The diffuse contribution of the disordered solvent molecules was described using the bypass (a.k.a. squeeze) option of the program package [44]. The main crystallographic data and structure refinement parameters are summarized in Table 1.

The full set of X-ray diffraction parameters was deposited with the Cambridge Crystallographic Data Centre (CCDC no. 2244205 (**I**) and 2244206 (**II**); deposit@ccdc.cam.uk).

The mathematical modeling of the probability of binding of Cu^{2+} cation to the amino acid residues of *M. smegmatis* proteins was carried out by rigid intermolecular docking using the MIB2 web server [46], including various methods for calculating the cation affinity to amino acids. The protein structures were taken from the UniProtKB open protein database. The docking results were analyzed by the PyMol molecular graphics system (Version 2.5.4, Schrödinger, LLC). The docked conformers were selected considering the following parameters: amino acid residues (>2; binding to the ion); bonds (>2; the bond should satisfy the covalent/ionic/coordination bond characteristics); rank (rating in the list of the identified complexes for each protein ranked from larger to smaller score function), and the score of the complex (>2; highest scores when the above conditions are met). Since the authors of MIB2 did not propose a clear procedure for interpreting the scores of the resulting complexes, the absolute scores were not taken into account in the comparison of the complexes and were interpreted qualitatively as the possibility or impossibility of binding. This condition was accepted to avoid a false interpretation of the docking results to minimize the probability of type I error, as the operation of MIB2 algorithm is based on a predictive model and is probabilistic. The docked complexes and bond parameters were validated using the PyMol software with the Show Contacts plug-in, which show the possible bonds of Cu^{2+} to N and O atoms in the amino acids of ion-binding sites.

RESULTS AND DISCUSSION

The synthesis included the ion exchange reaction of copper(II) acetate with furancarboxylic acid in acetonitrile (**I**)/methanol (**II**) with the subsequent addition of Nphen in methanol (Scheme 1).

Table 1. Crystallographic parameters and structure refinement details for the structures of **I** and **II**

Parameter	Value	
	I	**II**
Molecular formula	$C_{44}H_{28}N_6O_{17}Cu_2$	$C_{44}H_{22}N_{10}O_{24}Cu_2$
M	1039.80	1201.79
T, K	100	
System	Monoclinic	Triclinic
Space group	$P2_1/c$	$P\bar{1}$
Crystal size, mm; color	0.3 × 0.2 × 0.1; blue	0.2 × 0.1 × 0.1; turquoise
a, Å	12.6015(2)	8.8569(4)
b, Å	17.7797(2)	10.6206(5)
c, Å	9.71830(10)	12.9265(6)
α, deg	90	74.247(2)
β, deg	108.3560(10)	84.403(2)
γ, deg	90	76.162(2)
V, Å^3	2066.60(5)	1135.61(9)
Z	2	2
ρ(calcd.), g/cm^3	1.671	1.757
μ, mm^{-1}	1.118	1.044
F(000)	1056	606
Data collection range for θ, deg	2.05–26.00	2.043–25.494
R_{int}	0.0333	0.0340
Number of measured reflections	21234	11100
Number of unique reflections	4049	4219
Number of reflections with $I > 2\sigma(I)$	3609	3887
Number of refined variables	361	381
GOOF	1.017	1.087
R-factors on $F^2 > 2\sigma(F^2)$	$R_1 = 0.0256$, $wR_2 = 0.0646$	$R_1 = 0.0500$, $wR_2 = 0.1347$
R-factors for all reflections	$R_1 = 0.0304$, $wR_2 = 0.0666$	$R_1 = 0.0532$, $wR_2 = 0.1377$
Residual electron density (max/min), e/Å^3	0.432/–0.310	1.794/–0.707

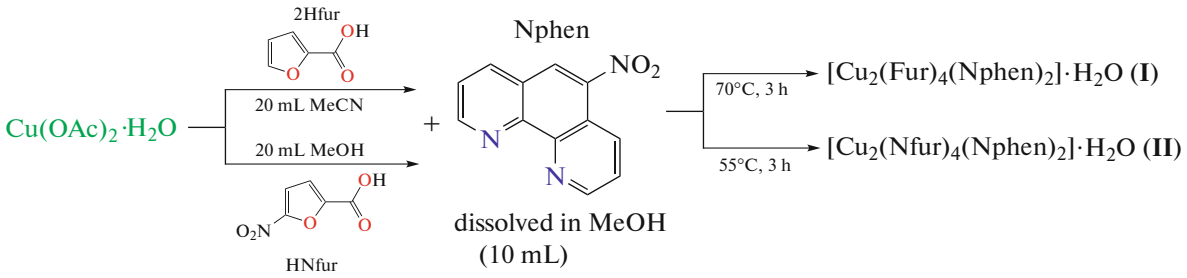

Scheme 1.

The first step gave a green suspension, and the subsequent addition of Nphen resulted in the formation of a blue transparent solution, which was kept for an additional 3 h and then filtered. Slow evaporation of the mother liquor yielded crystals suitable for X-ray diffraction.

Compound **I**, which is a molecular binuclear copper(II) complex, crystallizes in the monoclinic sys-

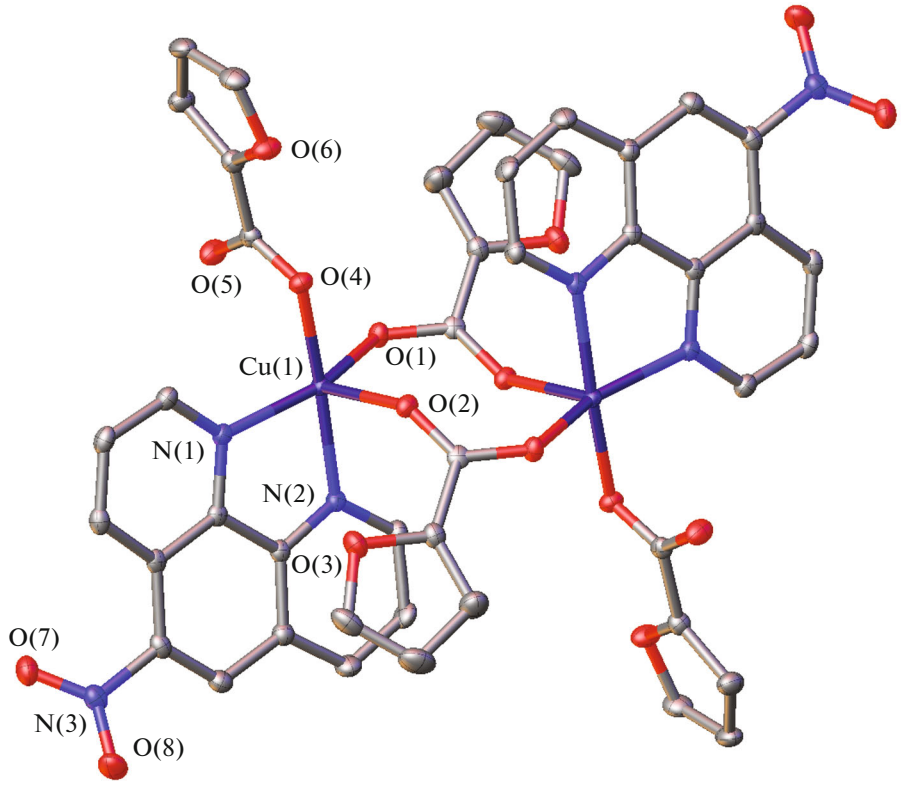

Fig. 1. General view of complex **I**. Hereinafter, hydrogen atoms (except for those belonging to water molecules) are not shown, non-hydrogen atoms are represented as thermal ellipsoids (p = 50%), and numbering is given only for heteroatoms of the independent part of the unit cell.

tem, space group $P2_1/c$, with one water molecule per one formula unit of the complex (Table 1). The complex in the crystal occupies a special position, with the inversion center coinciding with the center of the eight-membered metallacycle (Fig. 1). The coordination environment of the complex-forming metal ion is composed of two nitrogen atoms of the Nphen ligand and three oxygen atoms of three Fur^- anions and has the geometry of a distorted tetragonal pyramid, C.N.(Cu) is 5 (Fig. 1; selected bond lengths are summarized in Table 2). Two of the three Fur^- anions act as bridging ligands linking copper(II) atoms to each other, while the third one forms a hydrogen bond with the water molecule of solvation (O...O, 2.799(4) and 2.939(4) Å; OHO, 168(8)° and 170(5)°; Table 3). These hydrogen bonds connect the molecules of **I** into hydrogen-bonded chains in the crystal along the diagonal of the *a*0*c* crystallographic plane. In turn, the chains are combined into layers due to the stacking interactions between the parallel phenanthroline rings (the distance between the centroids is 3.4215(10) Å, the shift is 1.3313(14) Å) (Fig. 2, Table 3).

Complex **II** crystallizes in the triclinic system, space group $P\bar{1}$ (Table 1), and has a structure similar to that of **I** (Fig. 3, Table 2). Due to the absence of solvation water molecules, the main supramolecular units are infinite chains (Fig. 4) formed by stacking interactions between parallel aromatic rings of Nphen (the distance between the centroids is 3.558(2) Å; the shift is 1.347(3) Å) of neighboring molecules of the complex. They are additionally stabilized by a weak coordination bond (3.090(7) Å) between the Cu^{2+} ion and the oxygen atom of one of the components of the disordered nitro group of Nphen (Fig. 4, Table 2). Thus, unlike **I** in which the complex-forming ion has C.N. 5, in compound **II**, C.N.(Cu) is (5 + 1).

The UV-Vis spectra of **I** and **II** (2.5×10^5 M) were recorded in physiological saline (0.9% NaCl) for 48 h at room temperature (Fig. 5). Both compounds exhibit high absorption rates at high energy; the absorption bands at 275 nm correspond to intraligand transitions in the Nphen molecule, while low-intensity absorption bands at 300–350 nm are due to the metal-to-ligand charge transfer [47, 48]. According to the data of the absorption spectra, a salt solution of **I** is highly stable over time, whereas in a solution of **II**, a minor degradation takes place, associated with hydrolytic reactions in the complex with time. It is important that hydrolysis is more intense in the first six hours after dissolution of the compound, while in the rest 32 h the system occurs in a relative equilibrium.

Table 2. Selected bond lengths (*d*) and bond angles (ω) in the structures of **I** and **II***

Bond	*d*, Å	Bond	*d*, Å
I		**II**	
Cu(1)–O(4)	1.9313(12)	Cu(1)–O(1)	1.928(2)
Cu(1)–O(2)$^{1\#}$	2.1985(12)	Cu(1)–O(4)	1.937(2)
Cu(1)–O(1)	1.9417(13)	Cu(1)–O(2)$^{2\#}$	2.358(2)
Cu(1)–N(1)	2.0331(15)	Cu(1)–N(1)	2.014(3)
Cu(1)–N(2)	2.0192(15)	Cu(1)–N(2)	2.0149(3)
Cu(1)...Cu(1)$^{1\#}$	4.5653(4)	Cu(1)...O(11')$^{2\#}$	3.090(7)
		Cu(1)...Cu(1)^{1}	4.3003(9)
Angle	ω, deg	Angle	ω, deg
N(1)Cu(1)N(2)	81.18(6)	N(1)Cu(1)N(2)	81.08(12)
N(1)Cu(1)O(1)	155.14(6)	N(1)Cu(1)O(1)	165.45(11)
N(1)Cu(1)O(2)$^{1\#}$	98.62(5)	N(1)Cu(1)O(2)$^{2\#}$	88.85(10)
N(1)Cu(1)O(4)	92.60(6)	N(1)Cu(1)O(4)	91.24(11)
N(2)Cu(1)O(1)	98.9(6)	N(2)Cu(1)O(1)	87.90(11)
N(2)Cu(1)O(2)$^{1\#}$	88.62(5)	N(2)Cu(1)O(2)$^{2\#}$	93.54(10)
N(2)Cu(1)O(4)	171.72(6)	N(2)Cu(1)O(4)	172.31(11)

* Symmetry codes: $^{1\#}$ $-x, 1-y, -z$; $^{2\#}$ $1-x, -y, 1-z$.

Table 3. Geometric parameters of hydrogen bonds in the structure of **I**

D–H...A	Distance, Å			DHA angle, deg
	D–H	H...A	D–A	
O(9)–H(9)...O(5)	0.86(6)	1.95(6)	2.799(4)	168(8)
O(9)–H(9)...O(5)	0.91(6)	2.04(6)	2.939(4)	170(5)

The antibacterial activity of **I** and **II** was determined against the non-pathogenic *M. smegmatis* strain, which is a model for the virulent tuberculosis pathogen *Mycobacterium tuberculosis* (MTb, Koch's bacillus). It is known that the resistance of mycobacteria to chemotherapeutic agents is related to the low permeability and unusual structure of the mycobacterial cell wall. *M. smegmatis* is fast-growing non-pathogenic mycobacterium used to model the slowly growing *M. tuberculosis* and for the primary screening of antituberculosis drugs [49]. The *M. smegmatis* test system is more resistant to antibiotics and antituberculosis agents than MTb; therefore, the concentration <100 μmol/disc was used as the selection criterion [50]. All the in vitro biological activity data for the test compounds were compared with the activities of isoniazid (INH) and rifampicin (Rif) under the same experimental conditions. The compounds were applied onto the discs in various concentrations.

The data on the antibacterial activity against the *M. smegmatis* mc^2 155 test system and its variation with time for compounds **I** and **II** are summarized in Table 4. The prepared complexes with Nphen have high activity; in particular, **II** has the same efficiency as the previously prepared highly active [Cu(Fur)$_2$Phen] [34]; its activity is comparable with that of rifampicin. The activities of free ligands are several times lower than those of **I** and **II**. It should be noted that analysis of the halo area for **II** allowed us to elucidate the nature of the effect of compound **II** on the bacterial culture: the transparent zone around the disc was indicative of the bactericidal action of the complex; the bacterial growth inhibition zone was not overgrown after 120 h. Unlike **II**, compound **I** exhibited a bacteriostatic effect (the inhibition zone was overgrown over time). Thus the obtained complexes **I** and **II** are among the most active and promising out of the zinc, cobalt(II), copper(II), and nickel(II) compounds tested in relation to *M. smegmatis* [33–40].

The search for the possible ways of action of copper(II) cations on the protein molecules of the *M. smegmatis* strain and for the location of effects in the polypeptide chain was accomplished using the mathematical modeling by rigid intermolecular dock-

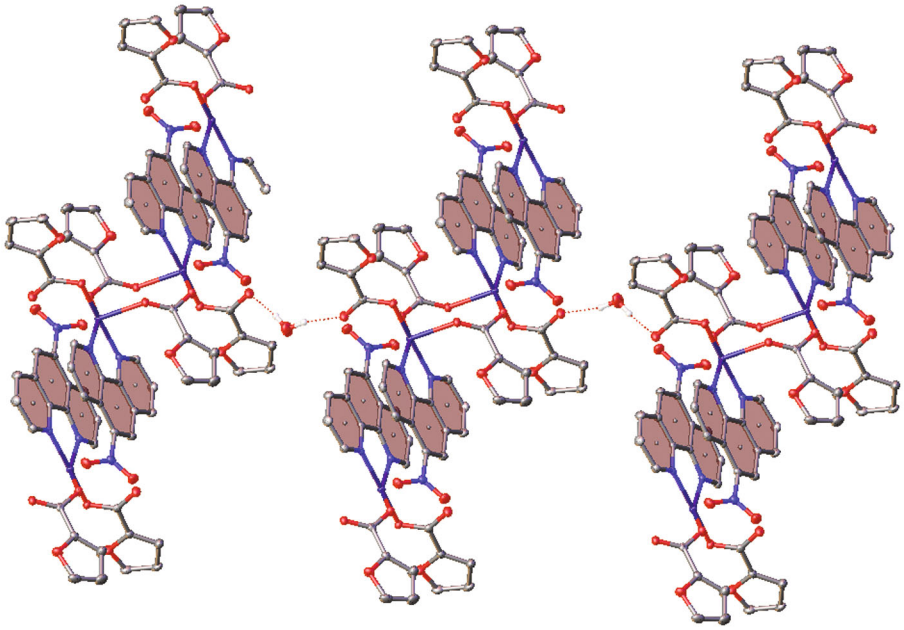

Fig. 2. Fragment of the crystal packing of **I**. The dashed lines show O–H...O hydrogen bonds; the planes of aromatic rings involved in the intermolecular stacking interactions are highlighted in dark color.

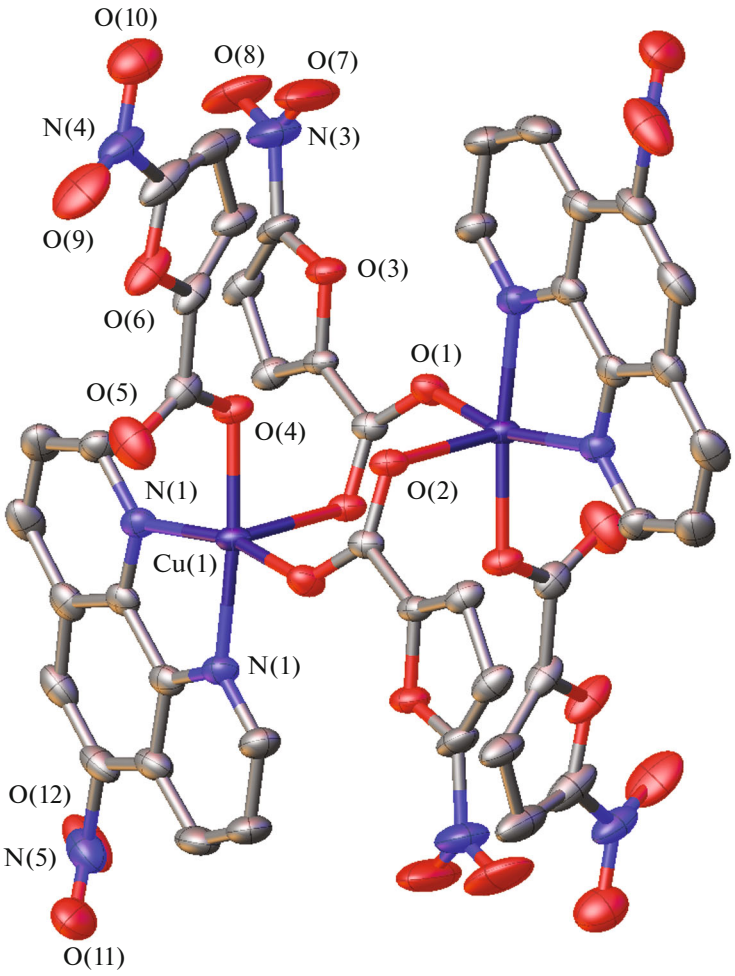

Fig. 3. General view of complex **II**. The minor components of the disordered nitro groups are not shown.

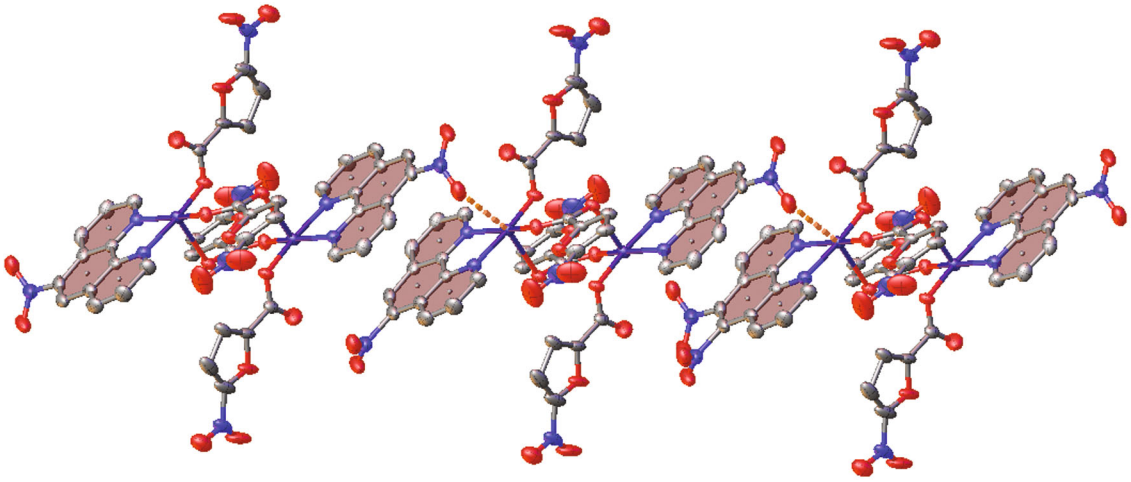

Fig. 4. Fragment of the crystal packing of **I**. The dashed lines show the additional Cu...O coordination bonds; the planes of aromatic rings involved in the intermolecular stacking interactions are highlighted in dark color.

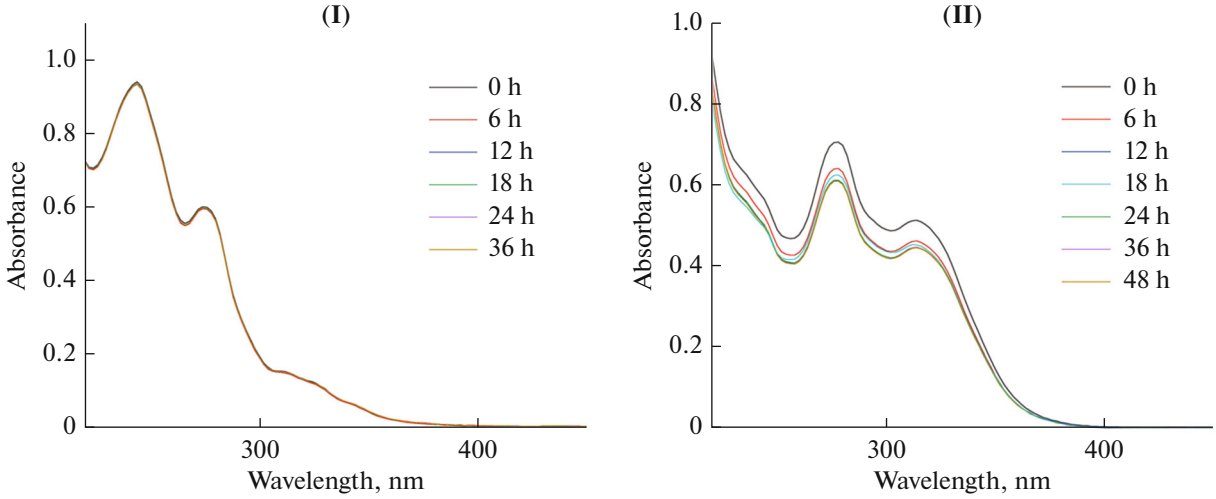

Fig. 5. UV-Vis spectra of **I** and **II** in physiological saline (0.9% NaCl) at 25°C.

ing. Figure 6 shows an example of a typical conformation of the protein with Cu^{2+}. The structure of the protein complex attests to potential binding to histidine (His) and arginine (Arg) nitrogen to give coordination bonds of 2.3–3.0 Å length and binding of the complex-forming metal to asparagine (Asp) oxygen (2.9 Å). The results of docking for some *M. smegmatis* proteins are summarized in Table 5. These data imply that the most frequently encountered amino acids in the protein polypeptide sites able to form coordination bonds are histidine (H, 7 of the total number of bonds for all proteins), glutamic acid (E, 5 times), and cysteine (C, 2 times), and single binding is found for arginine (R), glutamine (Q), serine (S), threonine (T), and aspartic acid (D). Analysis of the results of potential binding of the Cu^{2+} cation to amino acids revealed the formation of coordination bonds of different efficiency (2.3–3.7 Å); this confirms the adequacy of the procedure selected for validation of the results. In addition, Cys17 and Cys20 residues for the MSMEG_5014 protein and His68 and Cys72 residues for the MSMEG_0230 proteins are annotated ion-binding sites according to the NCBI database (https://www.ncbi.nlm.nih.gov/protein/ABK71068.1, MSMEG_5014 https://www.ncbi.nlm.nih.gov/protein/ABK69823.1, MSMEG_0230).

The cytotoxicity of complexes **I** and **II** was determined against *SKOV3* cells and *HDF* normal non-cancer cells used as a control. From the results of MTT assay, the IC_{50} value for each compound was calculated. The agents that cause the cancer cell death when present in low concentrations, while causing a minor effect on the viability of normal cells, are considered to be promising. The complexes in question proved to be ~2 more toxic to ovarian adenocarcinoma cells than to

Table 4. Data on the antibacterial activity in vitro for complexes **I** and **II** against *Mycolicibacterium smegmatis*

Compound	MIC, nmol/disc	Inhibition zone, mm		Ref.
	24 h	24 h	120 h	
I	10	7.0 ± 0.5	6.4 ± 0.17**	This work
II	5	6.5 ± 0.5	6.47 ± 0.17	This work
$[Cu(Fur)_2(Phen)]$	5	7.0 ± 0.5	7.0 ± 0.5	[29]
$[Cu_2(Fur)_4(Py)_2]$	200	7.0 ± 0.5	7.0 ± 0.5**	[29]
$[Cu(Fur)_2(Py)_2(H_2O)]$	400	7.0 ± 0.5	7.0 ± 0.5**	[29]
$[Cu(Fur)_2(Phpy)_2(H_2O)]\cdot Phpy$	250	7.0 ± 0.5	7.0 ± 0.5**	[33]
$[Cu(Fur)_2(NH_2\text{-}Py)_2]$	1000	7.0 ± 0.5	7.0 ± 0.5**	[33]
$[Cu_2(Fur)_4(MeCN_2)]$	187	7.0	7.0**	[34]
$[Cu(Fur)_2(Bipy)(H_2O)]$	100	7.0 ± 0.5	7.0 ± 0.5*	[30]
$[Cu(Fur)_2Neoc(H_2O)]$	25	6.7 ± 0.3	6.6 ± 0.1	[35]
$[Cu(Nfur)_2(H_2O)_2\cdot 2H_2O$	1000	6.7 ± 0.1	6.4 ± 0.1**	[36]
$[Cu(Nfur)_2(Py)_2(H_2O)]$	800	6.8 ± 0.3	6.6 ± 0**	[36]
$[Cu_2(Nfur)_4(Bipy)_2]\cdot H_2O$	20	7.0 ± 0.0	6.9 ± 0.1**	[36]
$[Co_3(Fur)_6(Phen)_2]$	50	7.0 ± 0.5	7.0 ± 0.5	[31]
$[Ni(Fur)_2(Phen)(H_2O)_2]\cdot H_2O$	484	6.7 ± 0.3	6.7 ± 0.3**	[32]
$[Zn(Fur)_2Neoc]$	101	7.1 ± 0.3	6.5 ± 0.5**	[35]
2HFur	1000	6.5		
HNfur	>1000			
Nphen	25	6.2 ± 0.2		
1,10-Phen	45	7.5 ± 0.5		
Neoc*	100	6.46 ± 0.06		
Bipy*	500			
INH	100	7.0 ± 0.5*	6.5 ± 0.5**	
Rif	5	7.2 ± 0.3	7.0 ± 0.0	

* Neoc is 2,9-dimethyl-1,10-phenanthroline (neocuproine) and Bipy is 2,2'-bipyridine.

** The growth inhibition zone of the bacterial culture, which initially appeared after a few hours of growth, begins to be overgrown over the entire surface.

healthy fibroblasts (Fig. 7, 8; Table 6). A comparison with cisplatin demonstrated that these complexes are more than two times more efficient against tumor cells, but also more toxic to healthy fibroblasts (selectivity index (SI) ~2). In comparison with the previously synthesized copper complex $[Cu_2(Fur)_4(MeCN_2)]$ [34], it should be noted that the introduction of Nphen increases the cytotoxic activity more than 30-fold for cancer cells and ~9-fold in comparison with the gold(III) complex, $(H_2Phen)[AuCl_4]Cl$ [41]. Thus, with further toxicity studies and selection of appropriate doses, the complexes may be considered as potential antitumor agents.

ACKNOWLEDGMENTS

X-ray diffraction studies were carried out using the research equipment of the Center of Molecular Structure Investigation at the Nesmeyanov Institute of Organoelement Compounds, Russian Academy of Sciences, supported by the Ministry of Science and Higher Education of the Russian Federation (state assignment no. 075-03-2023-642). Elemental analysis and IR spectroscopy studies were performed using equipment of the Center for Collective Use of Physical Investigation Methods of the Kurnakov Institute of General and Inorganic Chemistry, Russian Academy of Sciences.

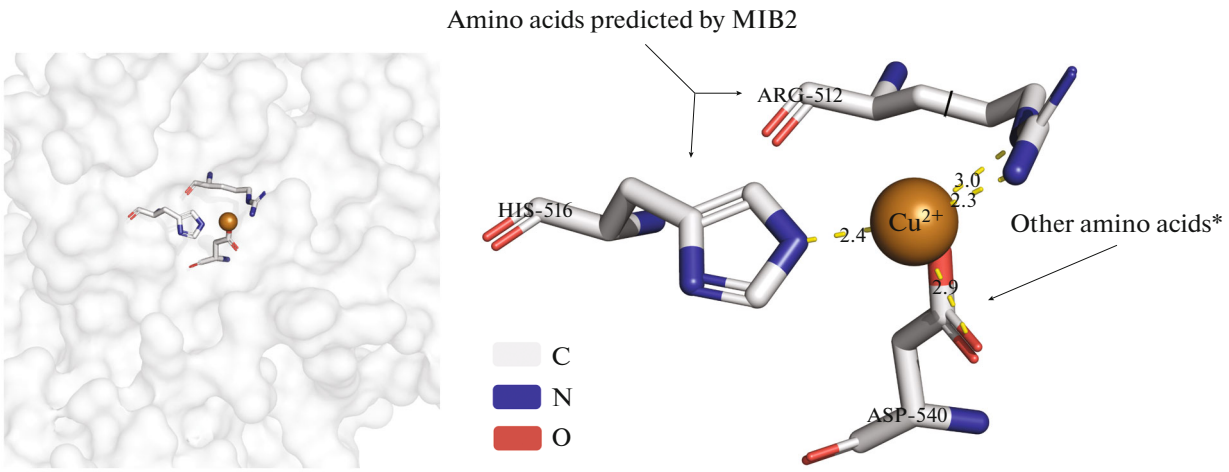

Fig. 6. Complex of the MSMEG_5636 protein with Cu^{2+}: (a) plan of the complex with a cavity for the cation in the protein structure; (b) isolated structure of the ion-binding site and Cu^{2+} with indicated amino acid residues and coordination bonds (dashed lines are shown in yellow); * amino acids potentially involved in cation binding (see Table 5).

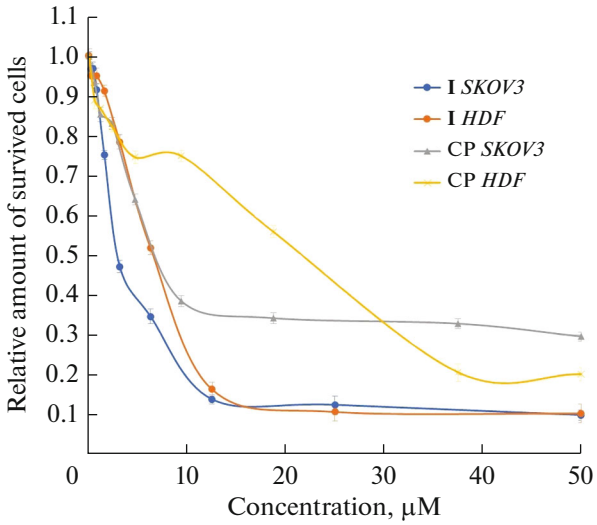

Fig. 7. Survival rate of *SKOV3* and *HDF* cells incubated with various concentrations of **I** or DMSO used as the control in comparison with cisplatin. The average MTT index ± standard deviation calculated from the results of three measurements is given.

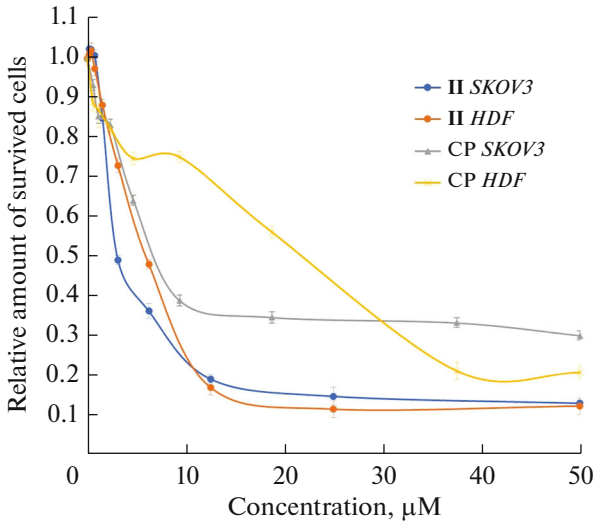

Fig. 8. Survival rate of *SKOV3* and *HDF* cells incubated with various concentrations of **II** or DMSO used as the control in comparison with cisplatin. The average MTT index ± standard deviation calculated from the results of three measurements is given.

Table 5. Results of MIB2 mathematical modeling

M. smegmatis (locus tag)	Cu^{2+}					
	rank	score	amino acids of the ion-binding site	other amino acids*	number of bonds	bond lengths, Å
MSMEG_5636	2	8.353	512R, 516H	540D	4	~2.3–3.0
MSMEG_0017	1	5.348	39Q, 42E	38H	3	~3.1–3.6
MSMEG_5014	4	4.730	17C, 20C (annotated)	16T, 20S	5	~3.2–3.6
MSMEG_6383	1	3.019	89H, 91H	34H, 82E, 102D	5	~2.6–3.7
MSMEG_0230	4	2.162	68H, 72C (annotated)		1	~3.3
MSMEG_5836	4	2.491	71H, 75E, 161E		3	~2.2–2.6

* Parameter determined by Show Contacts via PyMol.

Table 6. Data on the cytotoxic activity in vitro for complexes **I** and **II** against *SKOV3* and *HDF*

Compound	*SKOV3* IC_{50}, μM	*HDF* IC_{50} μM	SI	Ref.
I	2.9	6.5	2.3	This work
II	3.0	6.0	2.0	This work
$[Cu_2(Fur)_4(MeCN_2)]$	>100	55	<0.55	[34]
$(H_2Phen)[AuCl_4]Cl$	27.0	>150	5.6	[37]
CP	6.5	22.0	3.4	This work

FUNDING

This study was supported by the Russian Science Foundation (grant no. 22-13-00175).

CONFLICT OF INTEREST

The authors of this work declare that they have no conflicts of interest.

REFERENCES

1. Thompson, K. and Orvig, C., *Dalton Trans.*, 2006, vol. 6, p. 761.
2. Allardyce, C. and Dyson, P., *Dalton Trans.*, 2016, vol. 45, p. 3201.
3. Storr, T., Thompson, K.H., and Orvig, C., *Chem. Soc. Rev.*, 2006, vol. 35, p. 534.
4. Gregory, P., *Comprehensive Coordination Chemistry II: From Biology to Nanotechnology*, Oxford: Elsevier, 2005, vol. 9, p. 1062.
5. Jalal, M., Hammouti, B., Touzani, R., et al., *Mater. Today: Proceedings*, 2020, vol. 31, p. 122.
6. Hamza, A., Al-Sibaai, A.A., Alwael, H., et al., *Results Chem.*, 2022, vol. 4, p. 100422.
7. Li, J., Ren, G., Zhang, Y., et al., *Polyhedron*, 2019, vol. 157, p. 163.
8. Barry, N. and Sadler, P., *Chem. Commun.*, 2013, vol. 49, p. 5106.
9. Chan, W. and Wong, W., *Polyhedron*, 2014, vol. 83, p. 150.
10. Medici, S., Peana, M., Nurchi, V., et al., *Coord. Chem. Rev.*, 2015, vol. 284, p. 329.
11. Che, C.-M. and Siu, F.-M., *Curr. Opin. Chem. Biol.*, 2010, vol. 14, p. 255.
12. Dilruba, S. and Kalayda, G.V., *Cancer Chemother. Pharmacol.*, 2016, vol. 77, p. 1103.
13. Porchia, M., Pellei, M., Del Bello, F., et al., *Molecules*, 2020, vol. 25, p. 5814.
14. Ali, I., Mahmood, L.M.A., Mehdarassin, T.H., et al., *Inorg. Chem. Commun.*, 2020, vol. 118, p. 108004.
15. Zhang, Y., Zhou, Y., Zhang, H., et al., *J. Inorg. Biochem.*, 2021, vol. 224, p. 111580.
16. Pellei, M., Del Bello, F., Porchia, M., et al., *Coord. Chem. Rev.*, 2021, vol. 445, p. 214088.
17. Paprocka, R., Wiese-Szadkowska, M., Janciauskiene, S., et al., *Coord. Chem. Rev.*, 2022, vol. 452, p. 214307.
18. Viganor, L., Howe, O., McCarron, P., et al., *Curr. Top. Med. Chem.*, 2017, vol. 17, p. 1280.
19. Al-Omair, M.A., *Arab. J. Chem.*, 2019, vol. 12, p. 1061.
20. Ye, J., Ma, J., and Liu, C., *Biochem. Pharmacol.*, 2019, vol. 166, p. 93.
21. Simunkova, M., Lauro, P., Jomova, K., et al., *J. Inorg. Biochem.*, 2019, vol. 194, p. 97.
22. Gordon, A.T., Abosede, O., Ntsimango, S., et al., *Inorg. Chim. Acta*, 2020, vol. 510, p. 119744.
23. Eremina, J.A., Smirnova, K.S., Klyushova, L.S., et al., *J. Mol. Struct.*, 2021, vol. 1245, p. 131024.
24. Eremina, J.A., Ermakova, E.A., Smirnova, K.S., et al., *Polyhedron*, 2021, vol. 206, p. 115352.
25. Eremina, J.A., Lider, E.V., Kuratieva, N.V., et al., *Inorg. Chim. Acta*, 2021, vol. 516, p. 120169.
26. Eremina, J.A., Lider, E.V., Sukhikh, T.S., et al., *Inorg. Chim. Acta*, 2020, vol. 510, p. 119778.
27. Bravo-Gómez, M., Campero-Peredo, C., García-Conde, D., et al., *Polyhedron*, 2015, vol. 102, p. 530.
28. Davila-Manzanilla, S., Figueroa-de-Paz, Y., Mejia, C., et al., *Eur. J. Med. Chem.*, 2017, vol. 129, p. 266.
29. Correia, I., Borovic, S., Cavaco, I., et al., *J. Inorg. Biochem.*, 2017, vol. 175, p. 284.
30. Linder, M.C. and Hazegh-Azam, M., *Am. J. Clin. Nutr.*, 1996, vol. 63, p. 797.
31. Kaim, W. and Rall, J., *Angew. Chem., Int. Ed. Engl.*, 1996, vol. 35, p. 43.
32. Crichton, R.R. and Pierre, J.-L., *Biometals*, 2001, vol. 14, p. 99.
33. Lutsenko, I.A., Baravikov, D.E., Kiskin, M.A., et al., *Russ. J. Coord. Chem.*, 2020, vol. 46, no. 6, p. 411. https://doi.org/10.1134/S1070328420060056
34. Lutsenko, I.A., Yambulatov, D.S., Kiskin, M.A., et al., *Russ. J. Coord. Chem.*, 2020, vol. 46, no. 12, p. 787. https://doi.org/10.1134/S1070328420120040
35. Lutsenko, I.A., Yambulatov, D.S., Kiskin, M.A., et al., *Chem. Select.*, 2020, vol. 5, p. 11837.
36. Uvarova, M.A., Lutsenko, I.A., Kiskin, M.A., et al., *Polyhedron*, 2021, vol. 203, p. 115241.
37. Lutsenko, I.A., Kiskin, M.A., Koshenskova, K.A., et al., *Russ. Chem. Bull.*, 2021, vol. 70, no. 3, p. 463. https://doi.org/10.1007/s11172-021-3109-3

38. Lutsenko, I.A., Nikiforova, M.E., Koshenskova, K.A., et al., *Russ. J. Coord. Chem.*, 2021, vol. 47, no. 12, p. 879. https://doi.org/10.31857/S0132344X22020049

39. Lutsenko, I.A., Baravikov, D.E., Koshenskova, K.A., et al., *RSC Adv.*, 2022, vol. 12, p. 5173.

40. Koshenskova, K.A., Lutsenko, I.A., Nelyubina, Yu.V., et al., *Russ. J. Inorg. Chem.*, 2022, vol. 67, p. 1545. https://doi.org/10.31857/S0044457X22700106

41. Lutsenko, I.A., Loseva, O.V., Ivanov, A.V., et al., *Russ. J. Coord. Chem.*, 2022, vol. 48, p. 808. https://doi.org/10.1134/S1070328422700178

42. Naletova, I., Satriano, K., Cursi, A., et al., *Oncotarget*, 2018, vol. 9, p. 36289.

43. Pivetta, T., Trudu, F., Valletta, E., et al., *J. Inorg. Biochem.*, 2014, vol. 141, p. 103.

44. Sheldrick, G.M., *Acta Crystallogr., Sect. A: Found. Adv.*, 2015, vol. 71, p. 3.

45. Dolomanov, O.V., Bourhis, L.J., Gildea, R.J., et al., *J. Appl. Crystallogr.*, 2009, vol. 42, p. 339.

46. Lu, C.H., Chen, C.C., and Yu, C.S., *Bioinformatics*, 2022, vol. 38, no. 18, p. 4428. https://doi.org/10.1093/bioinformatics/btac534

47. Toigo, J., Farias, G., Salla, C.A.M., et al., *Eur. J. Med. Chem.*, 2021, vol. 31, p. 3177.

48. Liu, Y.-T., Yin, X., Lai, X.-Y., et al., *Dyes Pigm.*, 2020, vol. 176, p. 108244.

49. Ramon-García, S., Ng, C., Anderson, H., et al., *Antimicrob. Agents Chemother.*, 2011, vol. 8, p. 3861.

50. Bekker, O.B., Sokolov, D.N., Luzina, O.A., et al., *Med. Chem. Res.*, 2015, vol. 24, p. 2926.

Translated by Z. Svitanko